Journal of
NANOSTRUCTURES
JNS
NANOSTRUCTURES
JNS.kashanu.ac.ir

Synthesis and Characterization of Chitosan Coated Manganese Zinc Ferrite Nanoparticles as MRI Contrast Agents

M. Zahraei[a],*, A. Monshi[a], D. Shahbazi-Gahrouei[b], M. Amirnasr[c], B. Behdadfar[a], M. Rostami[d]

[a]*Department of Materials Engineering, Isfahan University of Technology, Isfahan 84156-83111, Iran*

[b]*Department of Medical Physics, School of Medicine, Isfahan University of Medical Sciences, Isfahan 81746-734615, Iran*

[c]*Department of Chemistry, Isfahan University of Technology, Isfahan 84156-83111, Iran*

[d] *School of Pharmacy, Isfahan Pharmaceutical Research Center, Isfahan University of Medical Sciences, Isfahan, Iran*

Article history:
Received 15/04/2015
Accepted 16/05/2015
Published online 01/06/2015

Keywords:
Mn-Zn ferrite nanoparticles
Hydrothermal
Chitosan
Ionic gelation
MRI contrast agents

**Corresponding author:*
E-mail address*:*
Zahraee_maryam@yahoo.com
Phone: +983133912750
Fax: +983133912752

Abstract

Manganese zinc ferrite nanoparticles (MZF NPs) were synthesized by using an efficient and environmental friendly hydrothermal method. To improve the colloidal stability of MZF NPs for biomedical applications, NPs were coated with chitosan by ionic gelation technique using sodium tripolyphosphate (TPP) as crosslinker. The synthesized NPs were characterized by XRD, ICP-OES, FTIR, TEM, VSM and DLS methods. Mean particle size of bare MZF NPs was around 14 nm. Chitosan coated NPs showed hydrodynamic size of 300 nm. The chitosan coated MZF NPs exhibited a positive surface charge across a wide pH range. All samples showed superparamagnetic-like behavior (zero remanence and coercivity) at room temperature. Furthermore, they were evaluated for imaging by measuring the relaxivities (r_1 and r_2). Chitosan encapsulated MZF NPs exhibited larger MRI contrast effects than that of commercial samples showing high potential to be applied as a MRI contrast agent.

1. Introduction

Magnetic nanoparticles (NPs) have been known as one of the nanostructures that provide the widest uses in biomedical applications such as magnetic resonance imaging (MRI), drug delivery, cellular signaling and hyperthermia [1-4].

Magnetic characteristics are crucial for the successful performances of magnetic NPs in biomedicine. Therefore, the development of new types of NPs is particularly important. In this regard, a

metal dopant substitution strategy of metal ferrite NPs has been pursued to achieve high and tunable nanomagnetism [5].

Jang and coworkers [6] have synthesized various metal-doped ferrite NPs and demonstrated that MnFe2O4 NPs have higher magnetic susceptibility, as compared with other divalent metal dopants. Also, it is very important to note that these NPs and their conjugates are non-toxic at examined concentrations. These metal-doped ferrite NPs with enhanced magnetic resonance contrast may be useful as ultrasensitive MRI probes.

This enhancement is significant for clinical purposes because the nanoparticle probe dosage level can be progressively lowered when using probes that have improved contrast enhancement effects [7]. Also, it was demonestrated that manganese zinc ferrite (MZF) NPs have superior MRI contrast effects that are larger than those of undoped Fe3O4 and MnFe2O4 NPs [6].

Control of particle size distribution and innovative functionalization techniques are also critical steps needed to effectively implement the use of magnetic NPs in medical applications [8-10]. Techniques such as hydrothermal offer an alternative to the commonly used co-precipitation method to produce magnetic NPs with a narrow size distribution and hence uniform magnetic properties [11].

Uncoated magnetic NPs aggregate in biological solutions due to their large surface area to volume ratio, forming large clusters and rending them unsuitable for biomedical applications. Therefore, an appropriate coating is needed to reduce the surface free energy in order to protect the NPs against agglomeration [12]. The polymer coating not only inhibits aggregation and increases stability but also leads to the creation of more hydrophilic nanostructures and provides a variety of surface functional groups to bind drug molecules [13].

Chitosan is a unique cationic, hydrophilic polymer that has beneficial properties such as low immunogenicity, excellent biodegradability as well as a high positive charge that easily forms polyelectrolyte complexes with negatively charged entities [12]. Chitosan is derived from the second most abundant natural polymer, chitin (major component of crustacean shells), by partial deacetylation in alkaline conditions. Its chemical formula (poly (1-4)-2-amino-2-deoxy-D-glucan) is shown in Fig. 1a [14].

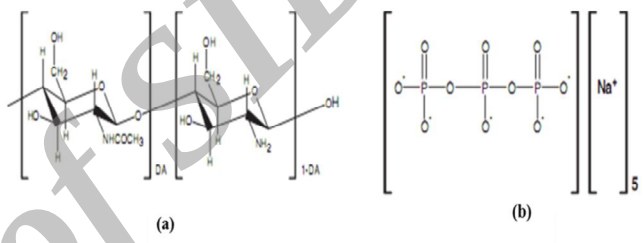

Fig. 1. Chemical formulas of (a) Chitosan (Ch); (b) Sodium tripolyphophate (TPP).

Due to its interesting functional groups (amino and hydroxyl) chitosan is widely used in biomedical applications [14]. In recent researchs, the magnetite–chitosan NPs were obtained by crosslinking of chitosan amino groups using glutaraldehyde [15, 16]. The disadvantage of this method is the toxicity of this crosslinker [14]. Ionic gelation (polyionic coacervation) is an interesting technique that uses non-toxic polyanions, such as sodium tripolyphosphate (TPP) (chemical formula shown in Fig. 1b) as non-toxic ionic crosslinker. This method is simple and reproducible and NPs are encapsulated in a chitosan shell by ionic interactions [14].

The main aim of this study is to synthesis of MZF NPs by using a direct, efficient and environmental friendly hydrothermal method. MZF NPs were subsequently coated with chitosan by ionic gelation using TPP as a crosslinker. Finally,

uncoated and coated MZF NPs were characterized by different analysis techniques such as X-ray diffraction (XRD), electron transmission microscopy (TEM), infrared (IR) and thermogravimetric analysis (TGA), vibrating sample magnetometery (VSM). Moreover, to study the efficiency of these agents for diagnostic, the NPs suspensions effects on MRI contrast were investigated by MRI relaxation time measurements.

2. Experimental procedure

2.1. Materials

Low molecular weight chitosan (degree of deacetylation=86.6%)and sodium tripolyphosphate (TPP) were purcased from sigma aldrich Co. All other chemicals, including FeCl3.6H2O, MnCl2.4H2O, ZnCl2 and NH4OH 25%, were purchased from Merck Co. with minimum purity of 99%. The water used in all experiments was double distilled.

2.2. NPs synthesis

To synthesis manganese zinc ferrite (MZF) NPs by hydrothermal method, stoichiometric amounts of $FeCl_3.6H_2O$, $ZnCl_2$ and $MnCl_2.4H_2O$ were completely dissolved in 25 ml distilled water to achieve 0.08, 0.11 and 0.17 molar concentration respectively. After 15 min stirring, a solution of NH_4OH 25% was added slowly to the medium to adjust the pH at 9.5. Vigorous stirring continued for another 10 min and a reddish brown slurry was formed. The mixed solution was poured into a Teflon lined stainless-steel autoclave (500 ml). Hydrothermal treatment was done at 180 ºC for 12h. The precipitate was washed with deionized water via magnetic decantation several times and then dried at 50 º C for 4h.

2.3. NPs encapsulation by Chitosan

Synthesised NPs were encapsulated in a chitosan shell by ionotropic gelation technique based on the interaction between the positively charged amino groups of chitosan and negatively charged phosphate groups of TPP.

To optimize of the fabricating conditions, the effect of Ch/TPP molar ratio on chitosan (Ch) NPs formation was firstly investigated. Briefly, 3 ml of chitosan solution (1 mg/ml) was prepared by dissolving chitosan in 0.1% w/v HCl solution until the solution was transparent. Solutions of sodium tripolyphosphate (TPP) in deionized water at different concentrations to obtain various molar ratios of Ch/TPP (1.5:1, 1.8:1, 2:1, 2.8:1) were prepared. The TPP solution was then flush mixed with chitosan solution and chitosan NPs formed spontaneously. To promote crosslinking, mild magnetic stirring at room temperature continued for 30 minutes. Then to remove excess unbounded chitosan and TPP, the resulting particles were washed several times by centrifugation and redispersion of precipitates in distilled water. To encapsulation of MZF NPs by using similar method, The MZF NPs suspension (3mg/mL) was first mixed with 3mL of chitosan solution (1 mg/ml chitosan in 0.1% w/v HCl) and the reaction mixture was vigorously stirred for 15 min. The TPP solution with optimized concentration was then flush mixed with chitosan solution and encapsulation of MZF NPs in chitosan–TPP NPs began spontaneously. For powder characterizations, the precipitate was freeze dried at -70 ºC and at pressure of 0.2 mbar. MZF NPs coated with chitosan were abbreviated as Ch-MZF.

2.4. Characterization

Phase identification was carried out using a Bruker diffractometer, D8ADVANCED model, with CuK_α radiation (λ=1.5406 A). Scherrer's formula ($d=0.9\lambda/B\cos\theta$) was used to estimate the mean

crystallite size (d) of the samples with full-width at half-maximum value (β) obtained from the spinel peaks [17]. Elemental analysis (ICP-OES) was used to quantify the final composition of the ferrites. Samples were first digested with nitric/chloridric acid. Particle and aggregation size were determined from TEM micrographs using a 200 keV JEOL-2000FXII microscope. For the observation of the sample in the microscope, a drop of diluted magnetic NPs suspension was placed on a carbon-coated copper grid. The mean particle size distribution were evaluated by measuring the largest internal dimension of at least 100 particles. Afterward, data were fitted to a log normal distribution by obtaining the mean size. Colloidal properties were characterized by dynamic light scattering (DLS) using a Malvern instrument Zetasizer (DTS Version 5.02) and 0.5 mM Fe NPs suspensions in water. Z-average values in intensity at pH of 7 were used as mean hydrodynamic size (D_H), and the Z potential was measured in a 0.01M KNO_3 solution. HNO_3 or KOH was added to the solution to alter the pH. Fourier transform infrared spectroscopy (FTIR) spectra were acquired using a Nicolet 20 SXC FTIR to confirm the ferrite phase, the nature of the coating and its surface bonding. IR spectra of the magnetic NPs were recorded between 4000 and 250cm^{-1}. Samples were prepared by diluting ferrite powder in KBr at 2% by weight and pressing them into pellets. Thermogravimetric analysis (TGA) was carried out in a Seiko TG/DTA 320U, SSC5200 to determine the weight percentage of polymer in the coated NPs. The analysis was performed from room temperature to 1000 ºC with an air flow. The magnetic properties of the samples were recorded in a vibrating sample magnetometer (Mag Lab VSM, Oxford Instrument). Hysteresis loops of the powder samples (pressed in a pellet) were measured at room temperature (RT) and 5K at the rate of 5kOe.min^{-1} .The saturation magnetization was evaluated by extrapolating the experimental data obtained in the high-field range to an infinite field; in the high-field range, the magnetization increases linearly with H, which can be approximated to a 1/H law.

To evaluate the efficiency of the hydrophilic suspensions as contrast agents, the relaxation times ($T_{1,2}$) were measured in a MinispecMQ60 (Bruker) operating at 37°C, with a magnetic field of 1.5 T. The relaxation rate $R_{1,2}$ values ($1/T_{1,2}$, s^{-1}), obtained from the relaxation times measured ($T_{1,2}$, s), were corrected by subtracting the water relaxation rate in the absence of contrast agent ($R°_{1,2}$, s^{-1}). Linear fitting of the data gives straight lines whose slopes are the relaxivities $r_{1,2}$ (s^{-1} mM^{-1}) related to the iron concentration [Fe] (mM) [18]:

$$R_{1,2} = R°_{1,2} + r_{1,2}[Fe] \quad (1)$$

3. Results and discussion

3.1. Synthesis and characterization of MZF NPs

MZF NPs were synthesised by a hydrothermal method described elsewhere [19] with some modifications. Experimental parameters were adjusted to reach a certain composition for optimizing magnetic properties ($Mn_{0.6}Zn_{0.4}Fe_2O_4$), minimize the formation of the secondary phases such as hematite and to obtain particles sizes over 10 nm, which has been reported to give rise to better relaxometric property [20].

X-ray diffraction pattern for obtained sample is shown in Fig. 2. Well-resolved diffraction peaks reveal good crystallinity with the typical broadness of nanosize particles. Diffraction peaks at 29.9°, 35.3°, 42.8°, 53.3°, 56.7°, and 62.2° can be indexed to cubic spinel phase (JCPDS file n° 086–1355) that is formed without any calcinations process after synthesis. Moreover, small peaks at 33.2° and 53.9º show the

presence of a neglible amount of hematite (α-Fe_2O_3) (JCPDS file n° 071–0469) in the sample. Table 1 shows the elemental ratios of Mn, Zn and Fe for MZF NPs in comparison with theoretical stoichiometric ratios.

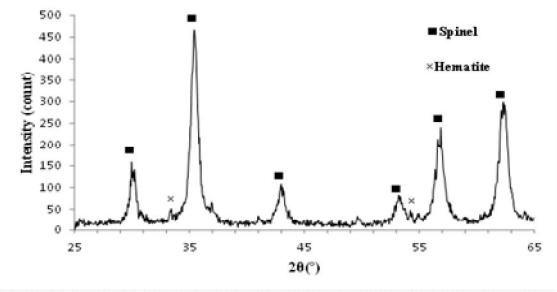

Fig. 2. XRD pattern of MZF NPs.

Fig. 3 shows the TEM image of the as synthesized MZF NPs. Mean particle size, which was calculated from TEM data, was 14 nm with a standard devition of 5nm (Fig. 3). As evidenced by Fig. 3, large agglomorations of NPs with a mean particle diameter of 14±5 nm form in accordance with DLS measurments which showed hydrodynamic size more than 2 µm with polydispersity index of 0.32.

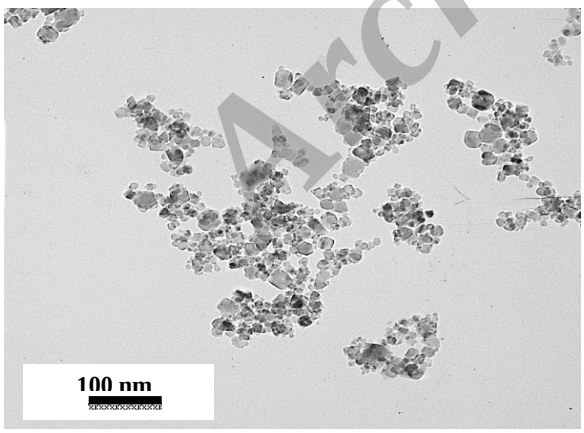

Fig. 3. TEM images of uncoated MZF NPs.

3.2. Fabrication and properties of chitosan and Ch-MZF NPs

Chitosan molecules are gelled when they encounter TPP molecules via electrostatic interaction [21]. Firstly, the zone of chitosan particle formation is investigated. By visual observation, the systems were classified as clear solution, opalescent suspension and aggregates. The results are summarized in Table 2. A clear solution was observed when both the chitosan and TPP concentrations were too small, where as aggregates were formed spontaneously when they were too large. The zone of the opalescent suspension, which should represent a suspension of colloidal particles, was found when the chitosan and the TPP concentrations were appropriate. Thus, Ch/TPP molar ratio of 2:1 was approprate ratio to Ch NPs formation and this ratio was selected for encapsulation of MZF NPs.

Table1. Elemental ratios for MZF NPs in comparison with theoretical stoichiometri ratios

Sample	Mn/Zn	Mn/Fe	Zn/Fe
Theoritical Mn0.6Zn0.4Fe2O4	1.50	0.30	0.20
MZF Synthesized in this wo	1.23	0.298	0.24

Table 2. Conditions for formation of the chitosan NPs.

Ch:TPP molar ratio	**1.5:1**	**1.8:1**	**2:1**	**2.8:1**
Solution col	aggregates	aggregates	opalescent	clear

Figs. 4 (a–c) show TEM images of chitosan encapsulated NPs (Ch-MZF) at different pH with different magnifications. As evidence from Fig. 4a, the dispersing behavior of Ch-MZF NPs has been improved in comparison with that of naked

NPs, which exhibits aggregated morphology (Fig. 3). The detail at higher magnification in Fig. 4 b confirms that at pH=3 several MZF cores agglomerated to form the chitosan encapsulated NPs. The layer of chitosan around the NPs can be observed from TEM image as a shadow. However, at around pH 7 the image (Fig. 4c) shows that Ch-MZF NPs quickly aggregate to form micrometric complexes in accordance with DLS measurments which showed hydrodynamic size of 950 nm with polydispersity index of 0.5.

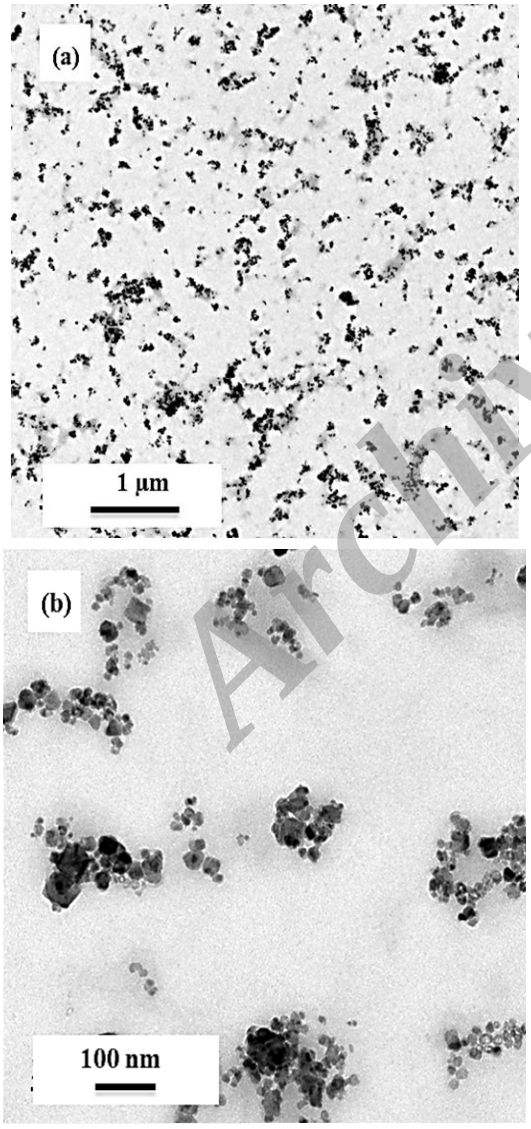

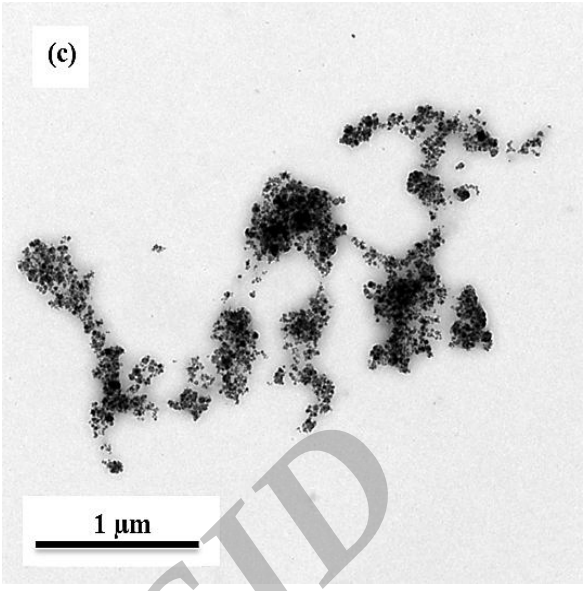

Fig. 4. TEM images of chitosan encapsulated NPs (Ch-MZF) at (a, b) pH=3 with different magnification and (c) pH=7.

To evaluate stability and aggregation degree after chitosan encapsulation, the colloidal properties of the hydrophilic suspensions were determined by measuring hydrodynamic size and polydispersity index (PDI) shown in Table 3 and zeta potential variation as a function of pH before and after polymer coating shown in Fig. 5. The unmodified magnetic NPs, precipitate in deionized water, according to their isoelectric point of charge that gives zero surface charge at pH around 7 (Fig. 5). The Ch-MZF NPs exhibited a positive surface charge across a wide pH range and the most positive charge and therefore maximum stability for the Ch-MZF NPs suspension was achieved at pH 3 (Fig. 4). The isoelectric point of the Ch-MZF NPs was found to be at pH 8.5.

Chitosan is known to be deprotonated at pH values above its pK_a (equal to 6.5), so it would be expected to precipitate in that pH range.

However, there are obviously stabilizing ionic forces exerted by TPP, strong enough to hold at elevated pH values and maintain the integrity of the chitosan encapsulated NPs [22].

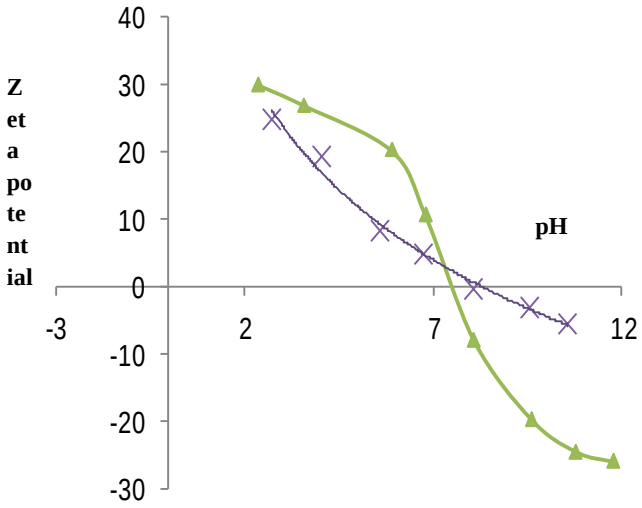

Fig. 5. Evolution of zeta potential of ▲: naked (MZF) and ×: chitosan encapsulated (Ch-MZF) MZF NPs as a function of pH.

For pharmaceutical applications, the storage stability and biocompatibility of the NPs is a great concern [21]. Here the storage temperature was kept constant at 23°C. It is worth mentioning that Ch-MZF NPs suspension can spontaneously precipitate after being store undisturbed for a couple of days. But they are very easily re-dispersed by gentle shaking.

The FTIR spectra of Ch and Ch-MZF NPs in comparision with pure chitosan and bare NPs are also shown in Fig. 6(a-d). A characteristic band at 3441 cm^{-1} is attributed to $-NH_2$ and –OH groups and the band at 1655cm^{-1} in Fig. 6a is characteristic of amide band. Where as in the FTIR spectrum of Ch and Ch-MZF NPs (Figs. 6b and 6c), the peak at 1655cm^{-1} disappears and two new peaks appear at 1645cm^{-1} and 1545 cm^{-1}. The disappearance of the band could be attributed to the linkage between the phosphoric and amine groups [23]. Bands in the region of 400–600 cm^{-1} are assigned to the metal skeleton vibrations (Figs. 6c and d) [24]. Appearance of both characteristic peaks of crosslinked chitosan and metal skeleton vibration in Fig. 5c can confirm succseccful modification of MZF NPs by chitosan.

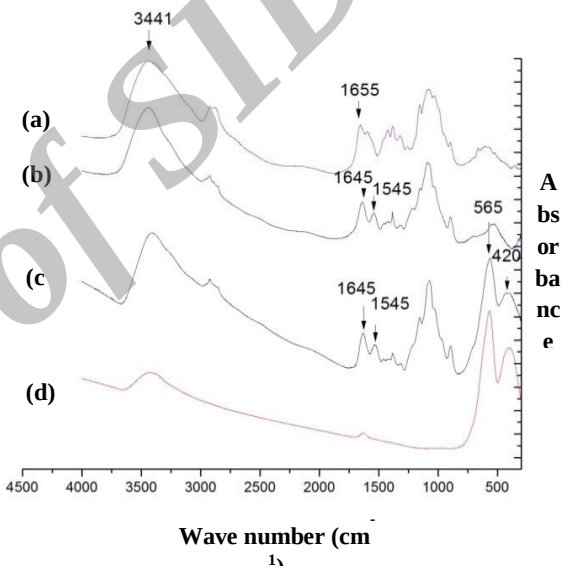

Fig. 6. FTIR spectra of (a) naked (b) Ch-MZF (c) Ch NPs and (d) pure chitosan.

The conjugation efficiency of polymer to the NPs surface was evaluated by quantifying the molecules bound to the NPs. TG analyses of MZF and Ch-MZF NPs (Fig. 7) reveal weight losses of 3 % and 34 % respectively.

All samples showed superparamagnetic-like behavior (zero remanence and coercivity) at room temperature (Fig. 8). Calculated saturation magnetization (M_s) of MZF and Ch-MZF are shown in Table 2.

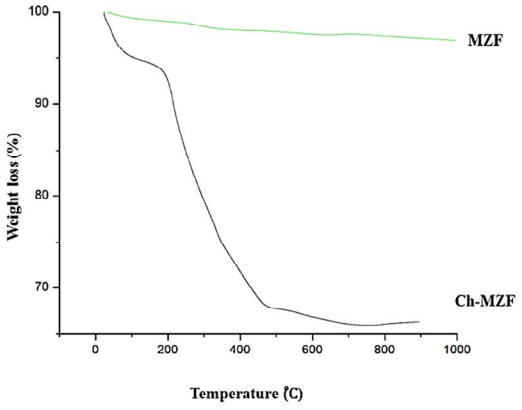

Fig. 7. TGA curves for MZF and chitosan-TPP encapsulated MZF NPs (Ch-MZF).

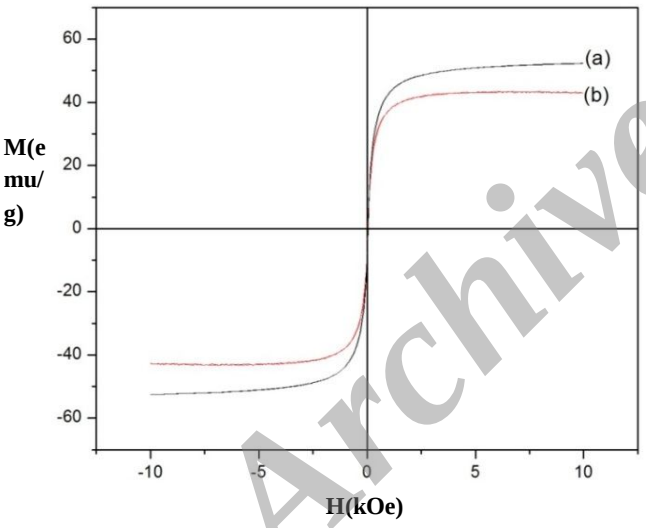

Fig. 8. M–H curve at room temperature for samples before and after coating. (a) naked and (b) chitosan encapsulated NPs.

strength used currently in clinical MRI were determind. Table 2 summarizes the measured relaxivity values of r_1 and r_2 which are defined as relaxation rates per concentration of Iron (Figs. 9a and b).

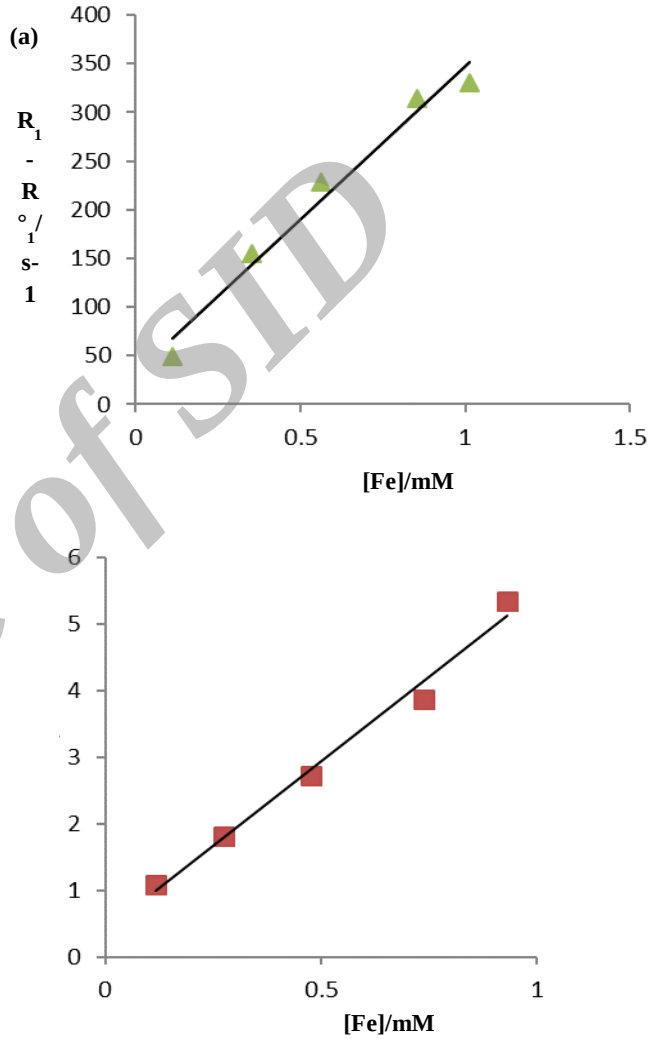

Fig. 9. (a, b): Inversion of the relaxation times as a function of the iron concentration for Ch-MZF NPs.

3.3. Evaluation of NPs as MRI contrast

To evaluate the effects of surface modified MZF NPs on the contrast in MR imaging, their longitudinal (R_1) and transverse (R_2) relaxation rates at 1.5 T, a typical field

Ch-MZF NPs showed much higher r_2 values (Table 3) than the published values for the commercial MRI contrast agent Endorem, and Resovist, both of which are prepared by

coprecipitation and have hydrodynamic sizes of 150 and 60 nm, respectively [25]. r_2 values <120 mM^{-1} s^{-1} are usually obtained for particles synthesized by coprecipitation, even for particle with mean size of 15 nm [26]. The magnetic moment in iron oxide based NPs is due to the localized electron density and hence strongly depends on the degree of crystallographic order [27]. As the hydrothermal synthesis of MZF NPs was performed at relatively high temperature and pressure compared to the alkaline coprecipitation method used for synthesis of commercial products, an improved crystallinity can be obtained [27]. Moreover, the substitution of Mn and Zn elements into ferrite structure is important to increase saturation magnetization of magnetic core [28]. These, in conjunction with the smaller core size and higher polydispersity of Endorem and Resovist explain the relatively higher relaxivities of our samples. This is a clear advantage for use in MRI imaging, since the dose can be reduced and technique sensitivity can be increased.

Table 3. Colloidal, magnetic and MR relaxometric properties of MZF and Ch-MZF NPs suspensions.

Sample	D_H (nm)	PDI	M_s (emu/g)	r_2 (mM/s)	r_1 (mM/s
MZF NPs	2750	0.32	62.5	*	*
Ch-MZF NPs	299	0.33	49.9	315.8	5.0

*It is not measured.

4. Conclusion

Crystalline MZF NPs with core size of 14nm were successfully synthesized by hydrothermal method and then MZF NPs were encapsulated in crosslinked chitosan by ionic gelation method to render them biocompatible and water dispersible. Chitosan encapsulated NPs with hydrodynamic size of 299 nm showed much higher r_2 value than the published values for the commercial MRI contrast agents as Endorem and Resovist which make them attractive for biomedical applications such as MRI contrast agents for cancer diagnostic.

Acknowledgments

This work was supported by the Isfahan University of Technology, Iran. Support on the characterization by the group of Biomaterials and Bioinspired Materials, Instituto de Ciencia de Materials de Madrid, Spain is gratefully acknowledged.

References

[1] H. Montazeri, A. Amani, H. R. Shahverdi, E. Haratifar and A. R. Shahverdi, J. Nanostructure Chem. 3 (2013) 1-6.

[2] H. Shokrollahi, Mater. Sci. Eng. C 33 (2013) 2476–2487.

[3] M. Mahmoudi, A. Simchi, M. Imani, J. Iran. Chem. Soc. 7 (2010) S1–S27.

[4] I. Hilger and W. A. Kaiser, Nanomedicine 7 (2012) 1443-1459.

[5] R. Raeisi Shahraki and M. Ebrahimi, J. Nanostructure 2 (2012) 413-416.

[6] J. T. Jang, H. Nah, J. H. Lee, S. H. Moon, M. G. Kim, and J. Cheon, Angew. Chem. Int. Ed. 48 (2009) 1234–1238.

[7] J. H. Lee,Y. M. Huh, Y. W. Jun, J. w. Seo, J. T. Jang,
H. T. Song, S. j. Kim, E. J. Cho, H. G.Yoon, J. S. Suh,
J. Cheon, Nat. Med. 13 (2007) 95–99.

[8] Q. A. Pankhurst, J. Connolly, S. K. Jones, J. Dobson, J. Phys. D: Appl. Phys. 36 (2003) R167-181.
[9] A. P. Herrera, C. Barrera, C. Rinaldi, J. Mater.
Chem. 18 (2008) 3650-3654.
[10] S. Mornet, J. Portier, E. Duguet, J. Magn. Magn. Mater. 293 (2005) 127-134.
[11] H. Eshtiagh-Hosseini, H. Aghabozorg, M. Shamsipur, M. Mirzaei and M. Ghanbari, J. Iran. Chem. Soc., 8(2011) 762-774.
[12] H. Arami, Z. Stephen, O. Veiseh, and M. Zhang, Adv. Polym. Sci. 243 (2011) 163–184.
[13] J. P. Chen, P. C. Yang, Y. H. Ma, T. Wu, Carbohydr. Polym. 84 (2011) 364–372.
[14] D. Hritcu, M. I. Popa, N. Popa, V. Badescu,V. Balan, Turk. J. Chem. 33 (2009), 785-796.
[15] R. M. Patil, P. B. Shete, N. D. Thorat, S. V. Otari, K. C. Barick, A. Prasad, R. S. Ningthoujam, B. M. Tiwale, S. H. Pawar, J. Magn. Magn. Mater. 355 (2014) 22–30.
[16] J. Qu, G. Liu, Y. Wang, R. Hong, Adv.Powder Technol. 21 (2010) 461–467.
[17] B. D. Cullity, Elements of X-ray Diffraction, second ed., Addison-Wesley, New York, 1996.
[18] A. Ruiz, G. Salas, M. Calero, Y. Hernández, A. Villanueva, F. Herranz, S. Veintemillas-Verdaguer, E. Martínez, D. F. Barber, M. P. Morales, Acta Biomaterialia 9 (2013) 6421-6430.
[19] Y. Xuan, Q. Li and G. Yang, J. Magn. Magn. Mater. 312 (2007) 464–469.
[20] I. Hilger and W. A. Kaiser, Nanomedicine 7 (2012) 1443-1459.
[21] H. Liu and C. Gao, Polym. Adv. Technol. 20 (2009) 613–619.
[22] P. Käuper, M. Forrest, Chitosan-based nanoparticles by ionotropic gelation, XIVth International Workshop on Bioencapsulation, Switzerland, 2006.
[23] D. R. Bhumkar and V. B. Pokharkar, AAPS Pharm. Sci. Tech. 7 (2006) E138-E143.
[24] A. G. Roca, J. F. Marco, M. P. Morales, C. J. Serna, J. Phys. Chem. 111 (2007) 18577–84.
[25] S. Laurent, D. Forge, M. Port, A. Roch, C. Robic, L.V. Elst, R. N. Muller, Chem. Rev.
108 (2008) 2064-2110.
[26] H. Amiri , R. Bustamante , A. Millán , N. J. Silva, R. Piñol, L. Gabilondo, F. Palacio, P. Arosio , M. Corti and A. Lascialfari, Magn. Reson. Med. 66 (2011) 1715–21.
[27] J. Huang, L. Bu, J. Xie, K. Chen, Z. Cheng, X. Li, and X. Chen, ACS Nano. 4 (2010) 7151–7160.
[28] B. D. Cullity, C. D. Graham, Introduction to magnetic materials, Wiley, New Jersey, 1996, 180 - 183.